Special Feature: CAE and Simulation

Research Report

Zero-dimensional Diesel Combustion Model and Its Application to the Transient Performance of a Multi-cylinder Engine

Matsuei Ueda, Kazuhisa Inagaki, Yusuke Takasu and Toshihiro Tani

Report received on Oct. 23, 2014

ABSTRACT The purpose of the present study is to investigate a diesel combustion model that is capable of predicting the transient performance of a diesel engine and a diesel engine system model by combining a combustion model and an engine control model. The latest diesel engine systems have become very complex to achieve lower fuel consumption and lower emissions so that the calibration of the engine control has become very complicated. In order to solve these problems, a new diesel combustion simulator (UniDES) was developed to evaluate diesel engine systems and transient performance. In order to obtain high calculation speed and high accuracy, UniDES uses a multi-zone model and a probability density function (PDF). Furthermore, the most recent version of UniDES introduced the sac pressure model in an injector and the spray interaction model for a swirl flow. Using these new models, the UniDES is capable of predicting aspects of engine performance, such as heat release rate and combustion noise, over the entire operation area. The engine performance predicted in the NEDC test cycle using UniDES+GT-POWER® and Matlab/Simulink® agreed closely with the experimental results. This simulation is expected to be a useful tool for the development and calibration of new engines.

KEYWORDS Diesel Combustion, Simulation, Transient, Control, Heart Release Rate, Engine System Development

1. Introduction

The advantages of diesel engines include good fuel consumption and high torque. In addition, automotive engineers are facing demands to further reduce emissions of diesel engines. As such, technologies such as high-pressure multiple-injection via a common rail system, exhaust gas recirculation (EGR), and an after treatment system have been adopted.[1,2] Due to the adoption of such new devices, the control parameters of the engine system are increasing, which makes it very difficult to evaluate the system and calibrate the parameters.[3]

One recent trend is the application of combustion and engine system simulation to resolve these problems. One example related to diesel combustion is three-dimensional computational fluid dynamics (3D-CFD), which facilitates detailed analysis of spray combustion.[4] However, 3D-CFD cannot be applied to transient conditions due to the calculation time required. In order to simulate transient conditions, the computation time must be no more than a few seconds for a single combustion cycle. Zero-dimensional (0D) or one-dimensional (1D) simulation methods are capable of rapid combustion calculation and can therefore be applied to transient conditions.[5-7] Note that the heterogeneity of the mixed gas in the cylinder must be considered in 0D or 1D simulations.

A new 0D diesel combustion simulation method, called UniDES, which is capable of calculating the heterogeneity of mixed gas in a cylinder, has been investigated. Since UniDES uses a multi-zone model and a probability density function (PDF), the calculations are fast and the simulations are accurate.[8] The present paper describes actual development applications of this model, focusing on the expansion of the operation range of the model to include the New European Driving Cycle (NEDC). The present paper also describes research into simulations incorporating a model to perform control functions equivalent to those of the electronic control unit (ECU) in actual engines.

© Toyota Central R&D Labs., Inc. 2014

2. Model Configuration

2. 1 Combustion Model

The UniDES model achieves higher prediction accuracy through its unique spray and air-fuel mixture model structure. As shown in **Fig. 1**, the UniDES model treats combustion in the cylinder as a spray zone and an air zone. In addition, a probability density function (PDF) in the spray zone reveals the equivalence ratio and temperature inhomogeneity within the spray. **Table 1** shows a summary of the models in UniDES. Combinations of these models make it possible to calculate the heat release rate, torque, exhaust temperature, NOx, and so on. In addition, soot generation is predicted by the Hiroyasu soot model.[9] Moreover, the calculation time per combustion cycle was reduced to one second or less by optimizing the calculation code.

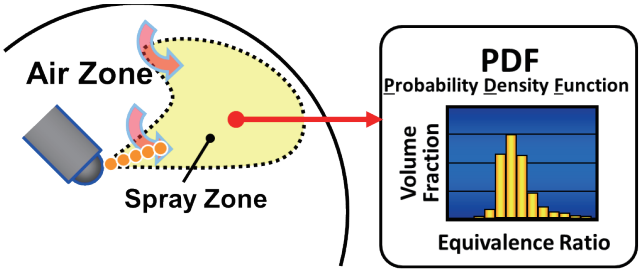

Fig. 1 Zone and probability density function (PDF) models.

Table 1 Summary of models used in UniDES.

Multi-injection process	Multi-zone model
Local inhomogeneity of mixture	PDF model
Air entrainment	Hiroyasu model[10]
Droplet size	Kawamura's equation[12]
Droplet evaporation	Spalding model[13]
Ignition	Multi-step shell model[14]
Combustion	Kong model[15]
Turbulence	Ikegami model[16]
Bulk flow (swirl/squish flow)	Arai model[17]
NOx	Extended Zeldovich model
Fuel injection rate	Double orifice model

As shown in **Fig. 2**, the multi-zone model, which is important for combustion prediction, can be described as follows. The spray zone is sub-divided into two regions, namely, zones 1 and 3. When fuel is injected into a cylinder, zone 1 is formed as the spray zone. The entrained air volume is calculated using the Hiroyasu equation.[10]

The ignition timing in zone 1 is defined as that at which the temperature of zone 1 exceeds 1000 K prior to the start of ignition. The details of the ignition model are described in a previous publication.[8] Once ignition occurs, zone 3 is formed, and air and fuel droplets are introduced to zone 3. The diffusive combustion is calculated in zone 3.

Furthermore, zones 4 and 5 are formed by the first and second pilot injections. Zones 6 and 7 are also formed for the two injections after the main injection. Overall, UniDES comprises seven zones. The gas of each zone is entrained into the spray zone not only from the air zone (zone 2), but also from the other spray zones, as shown in Fig. 2. In the present study, the percentage of the gas originating in the pilot and air zones in the total entrained gas is given in proportion to each volume fraction for the pilot and air zones.

A PDF was chosen to explain the inhomogeneity in the zones. In this PDF model, the mixture within each zone is treated as a cluster of discrete mixture fragments, called packages. The details of the PDF model were described in previous publications.[5,8]

2. 1. 1 Nozzle Sac Pressure Estimation

Pilot injections are generally small in quantity and

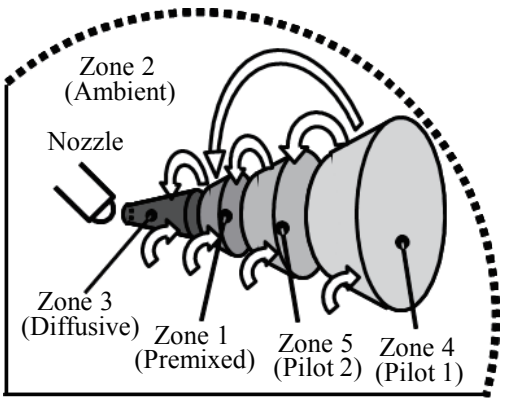

Fig. 2 Interactions between zones.

© Toyota Central R&D Labs., Inc. 2014

terminate before the sac pressure at the edge of the nozzle reaches the common rail pressure. Even for large injection quantities, such as main injections, the drop in the injection rate is due primarily to throttling of the nozzle seat. As shown in **Fig. 3**, a model that considers throttling at two points, i.e., the needle seat and the nozzle hole, is used in the present study.[11]

Converting the in-nozzle flow into a one-dimensional model yields the result shown on the right-hand side of Fig. 3. Here, P_{cr} is the rail pressure, P_{nzl} is the upstream seat pressure (= P_{cr}), P_{sac} is the sac pressure, P_{air} is the atmospheric pressure, A_s is the cross-sectional area of the seat channel, A_h is the total cross-sectional area of the nozzle hole, C_s is the seat flow coefficient, C_h is the nozzle hole flow coefficient, d_0 is the nozzle hole diameter, and α is the angle of the nozzle seat. When Bernoulli's equation is applied to a one-dimensional flow, the volume of fuel flow dQ per unit time is as follows:

$$dQ = C_s \cdot A_s \sqrt{\frac{2(P_{cr} - P_{sac})}{\rho_{fuel}}} = C_h \cdot A_h \sqrt{\frac{2(P_{sac} - P_{air})}{\rho_{fuel}}} , \quad (1)$$

where ρ_{fuel} is the fuel density, and A_s and A_h are obtained from their geometric shapes using the following equations:

$$A_s = \pi \cdot D_s \cdot L_N \cdot \cos(\alpha) , \quad (2)$$

$$A_h = 0.25 \cdot \pi \cdot d_0^2 \cdot n , \quad (3)$$

where L_N is the needle lift profile, n is the number of nozzle holes, and D_s is the seat diameter. Based on Eq. (1), the sac pressure is expressed as follows:

$$P_{sac} = \frac{(C_s \cdot A_s)^2}{(C_s \cdot A_s)^2 + (C_h \cdot A_h)^2} P_{cr} , \quad (4)$$

and the final dQ calculation is obtained as follows:

$$dQ = \frac{(C_s \cdot A_s)(C_h \cdot A_h)}{\sqrt{(C_s \cdot A_s)^2 + (C_h \cdot A_h)^2}} \sqrt{\frac{2P_{cr}}{\rho_{fuel}}} . \quad (5)$$

The injection period (τ) is obtained by starting with an initial value and repeating the calculation until the value matches the total injection quantity (Q). In order to calculate the cross-sectional area of the flow channel (A_s), the needle lift profile (L_N) must be known. L_N shown in **Fig. 4** was calculated based on the measurement and formulation of the opening and closing needle velocity (V_N).

Since Hiroyasu's equation requires a fixed value for the sac pressure (P_{sac}), a time-based average was used:

$$\overline{P}_{sac} = \left(1/\tau\right) \cdot \int_0^\tau P_{sac} dt . \quad (6)$$

Fuel droplet evaporation is expressed by the discrete droplet model (DDM).[5] The fuel injection rate was obtained as follows:

$$dm/dt = \rho_{fuel} \cdot dQ/dt . \quad (7)$$

2. 1. 2 Interaction of Adjacent Sprays under High-load Conditions

Under high-load operating conditions, in which the fuel injection period is long, the interaction between adjacent sprays due to the effect of swirl flows cannot be ignored. In order to expand the application of UniDES to high-load conditions, new models that

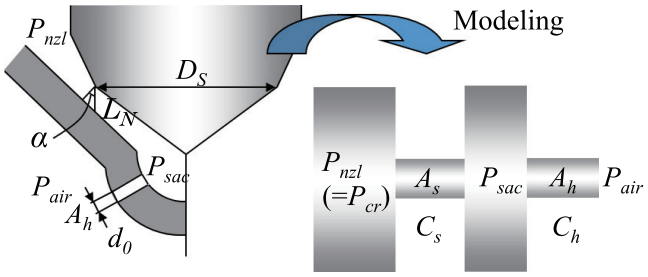

Fig. 3 In-nozzle flow model considering two throttling parts around needle-seat area and nozzle hole.

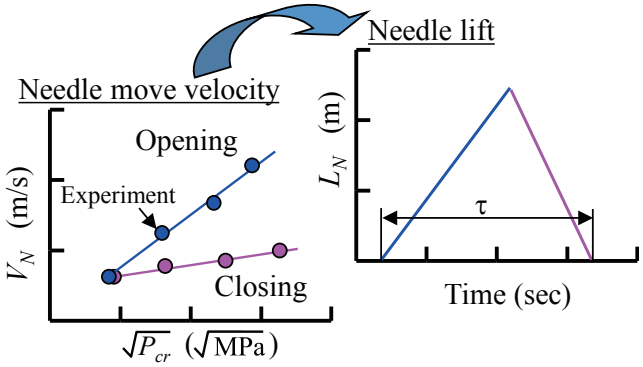

Fig. 4 Graphical images of procedure for calculating needle lift profile (L_N) and resultant injection period (τ) based on needle movement velocity (V_N) from common rail pressure.

© Toyota Central R&D Labs., Inc. 2014

consider the effect of this interaction were developed.

In the case of multi-hole injectors, spray flames are initially independent. However, the swirl flow causes these spray flames to reach the adjacent downstream spray. This obstructs the growth of the flame in the direction of the swirl, which causes a large drop in the heat release rate.

This effect was modeled as described below. **Figure 5** illustrates the sprays assumed by UniDES. The spray tip in the radial direction is calculated using Hiroyasu's penetration equation, and when the breakup length is exceeded, the spray tip is directed to the circumferential direction by the swirl.

In this case, the following equation is obtained using polar coordinates to represent the spray edge velocity (v_θ) in the circumferential direction:

$$v_\theta = \gamma \cdot r \cdot \omega_{swirl}, \tag{8}$$

where r is the distance of the edge of the spray from the center to the radius, and γ and ω are the tracking rate of the edge of the spray relative to the swirl flow and the swirl angular velocity, respectively, which are defined as follows:

$$\gamma = \begin{cases} 0 & (0 \le r < L_{core}) \\ 1 & (r \ge L_{core}) \end{cases} \quad \omega_{swirl} = \begin{cases} \omega_1 & (0 \le r < R_{cav}) \\ \omega_2 & (r \ge R_{cav}) \end{cases}, \tag{9}$$

where R_{cav} is the cavity radius. Using Arai's equation, ω_{swirl} is defined in terms of angular velocities ω_1 and ω_2 by the in-cylinder region into the cavity and squish area, respectively. The breakup length L_{core} is defined as follows:

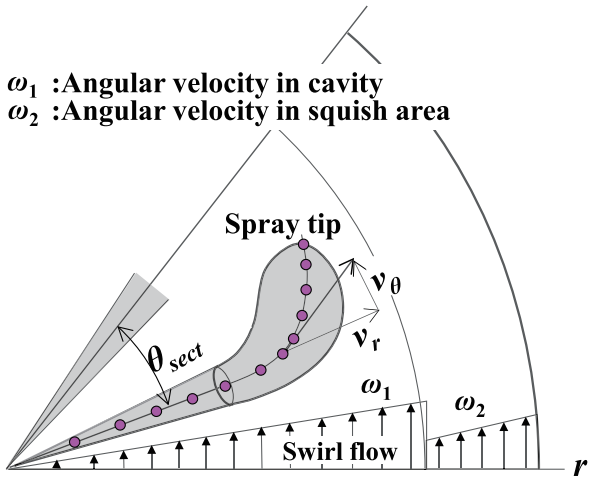

Fig. 5 Conceptual diagram of adjacent sprays interaction model.

$$L_{core} = 15.8 \cdot d_0 \sqrt{\frac{\rho_{fuel}}{\rho_{air}}}, \tag{10}$$

where ρ_{air} is the atmospheric density. The following equation represents the angle of motion θ_{spray} of the edge of the spray towards the swirl:

$$\theta_{spray} = {}^{1}\!/_{r} \cdot \int_0^t v_\theta dt. \tag{11}$$

For a single spray, the sector angle is defined as θ_{sect} (= $2\pi/n$, where n is the number of holes). During the injection period, when θ_{spray} exceeds $2\pi/n$, the adjacent spray has been reached and overlapping has occurred. After the adjacent spray is reached, the effect of entrainment obstruction by adjacent sprays was modeled by multiplying the amount of air entrained into the spray dV_{base} as derived from Hiroyasu's equation by a correction factor c ($0 < c < 1$), as follows:

$$dV = \begin{cases} dV_{base} & (\theta_{spray} \le \theta_{sect}) \\ c \cdot dV_{base} & (\theta_{spray} > \theta_{sect}) \end{cases}. \tag{12}$$

2. 2 Total Vehicle Model

As shown in **Fig. 6**, a total car model was constructed by combining an engine model, ECU model, vehicle model, and driver model. The GT-POWER® engine simulation tool was used to build the total car model, and UniDES was used in the combustion model of the engine model. When the intake valve is closed, the in-cylinder conditions, i.e., the pressure, temperature, gas composition, and the like, are input from GT-POWER® to UniDES. Then, UniDES calculates the combustion and in-cylinder conditions. The in-cylinder conditions

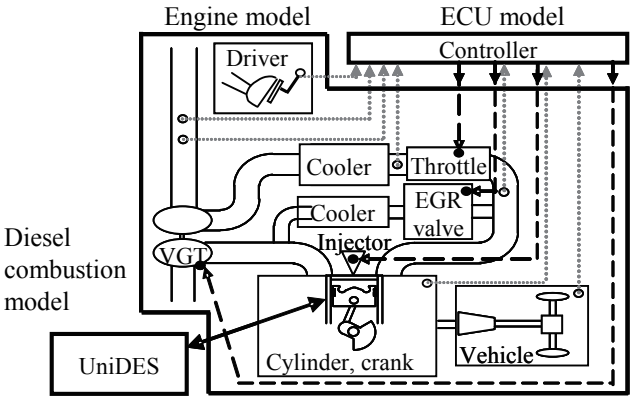

Fig. 6 Relationship between the models.

© Toyota Central R&D Labs., Inc. 2014

when the exhaust valve opens are input from UniDES to GT-POWER®, which then calculates the engine gas flow using a 1D fluid analysis code. Furthermore, the vehicle model models the inertia, and the load of the car is constructed in GT-POWER®.

The throttle, EGR valve, fuel injection pressure, number of injections, timing and quantity of each injection, and the other actuators in the GT-POWER® model are controlled by the ECU model. The accelerator pedal is controlled by the driver model, and the acceleration is input to the ECU model. The control logic used in the ECU model was coupled through Matlab/Simulink® to allow application of the model to various operating conditions. The ECU model automatically determines the actuator position and the fuel injection parameters from the engine speed and air flow obtained from the engine model.

3. Engine Specifications

Table 2 shows the specifications of the engine model used in the present study.

4. Results

4. 1 Nozzle Sac Pressure Estimation

Figure 7 shows the sac pressure prediction accuracy when the injection quantities and injection pressures were varied. The actual measured value is given for the hole flow coefficient (C_h). Since actual measurement of the seat flow coefficient (C_s) is difficult, the sac pressure was set to match the actual measurements as an adjustment parameter. In Fig. 7, the results are similar for all conditions, thereby demonstrating the effectiveness of the model.

Figure 8 compares the calculation results with the measured pilot spray penetration value obtained by shadowgraph visualization. With an injection quantity of 2.4 mm^3, the measurements and calculations with the model for estimating the nozzle sac pressure were similar under both injection pressure conditions. In contrast, the penetration was over-predicted when the common rail pressure was set as the sac pressure. Consequently, this model can be used to improve the accuracy with which the pilot spray self ignition properties and subsequent main spray ignition properties can be determined.

Figure 9 shows the heat release rates for a multiple-injection strategy consisting of the pilot injection, the main injection, and the after-injection. The graph on the right shows the results obtained using the nozzle sac pressure estimation model. The graph on the left shows the results obtained without this model, using the common rail pressure to represent the nozzle

Table 2 Engine specifications.

	Single cylinder	Multi-cylinder
Displacement volume	0.75 L	2.5 L
Number of cylinders	1	4
Stroke	4	4
Injection	Multiple injection	Multiple injection
Actuators	-	Variable geometry turbo
	-	EGR cooler with bypass
	-	EGR valve
	-	Throttle
Transmission	-	5MT

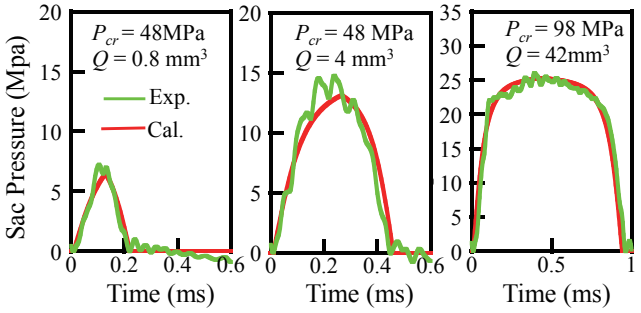

Fig. 7 Accuracy of sac pressure estimated by proposed model under three different injection conditions.

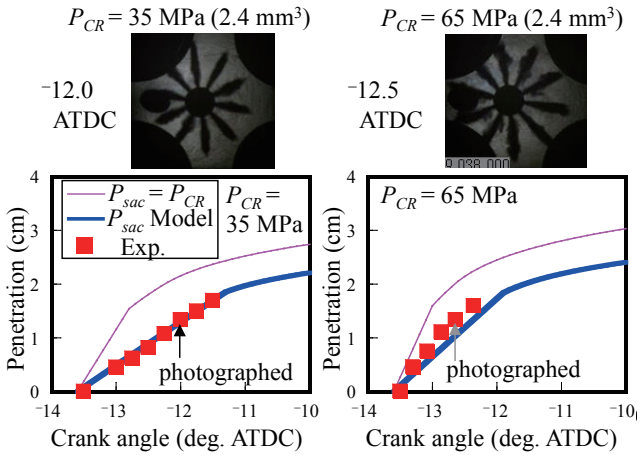

Fig. 8 Comparison of pilot spray penetration between calculation with and without model for estimating nozzle sac pressure, and visualized shadowgraph data using optical engine (engine speed: 1000 rpm, fuel quantity: 2.4 mm^3).

© Toyota Central R&D Labs., Inc. 2014

sac pressure and the rectangular injection rate. With a rectangular injection rate, the pre-mixture combustion spike is over-predicted. In addition, the pilot injection peak value and the post-injection ignition timing and peak value do not match the experimental results. In contrast, when this model was used, better heat release rates were obtained, and the obtained results were similar to the experiment results.

4. 2 Adjacent Spray Interaction

Figure 10 shows the heat release rates. The top figure shows the results obtained with the spray interaction model and the bottom figure shows the results obtained with the original UniDES model, which does not use an interaction model. The results obtained with the spray interaction model (top of Fig. 10) agree with the experimental results. In contrast, the results obtained using UniDES without the spray interaction model do not agree with the experimental results. In particular, the calculated heat release rates between 10 and 25 deg. ATDC are higher than the experimental results, whereas those between 25 and 60 deg. ATDC are lower than the experimental results (bottom of Fig. 10).

Figure 11 shows the spray pattern based on the results obtained using UniDES with the spray interaction model (top of Fig. 10). The sprays are rendered as time-lapse circles centered on the spray edge position calculated as a time integral in Eq. (8). The diameter of the circles is the spray width calculated based on the spay angle equation. Although not representing the actual shape of the spray, the circles can be used to trace the trajectory of the points having a high probability

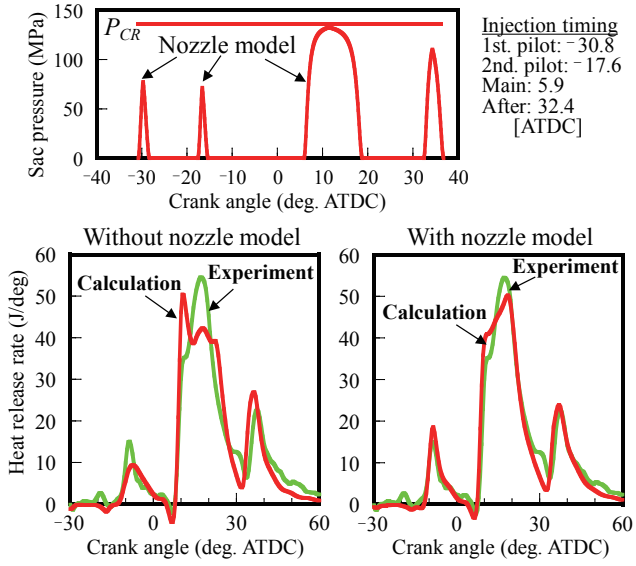

Fig. 9 Effect of nozzle sac pressure model on heat release rate in multiple-injection strategy (top: sac pressure history determined by nozzle model, left: without model, right: with model, engine speed: 2200 rpm, fuel quantity: 36 mm³, EGR ratio: 20%).

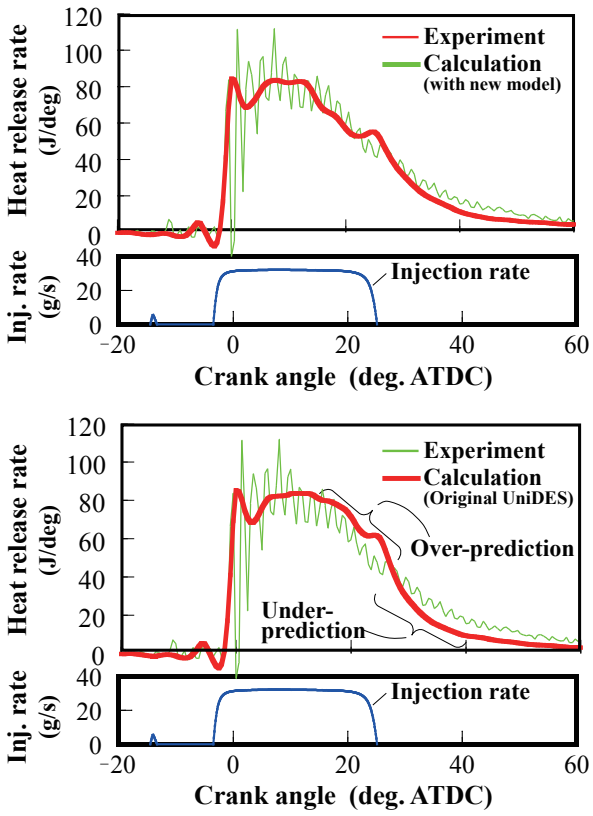

Fig. 10 Heat release rate at full load (top: with adjacent-spray interaction model, bottom: original UniDES, 2000 rpm, fuel quantity: 60 mm³) .

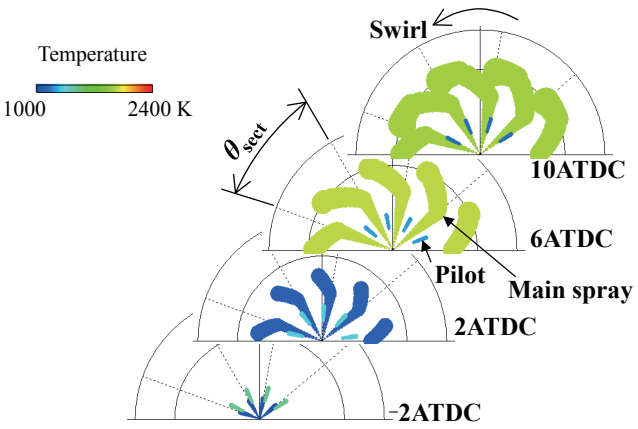

Fig. 11 Screen copy of spray-development graphics depicted by UniDES (same conditions as in Fig. 10).

© Toyota Central R&D Labs., Inc. 2014

of containing spray. As shown in Fig. 11, the time at which the spray at the top of the swirl reaches the injection axis of the adjacent spray is 10 deg. ATDC, after which the spray interaction starts. By taking the spray interaction into consideration in UniDES, it was capable of correctly predicting the heat release rates after 10 deg. ATDC (top of Fig. 10).

4. 3 Prediction of Multi-cylinder Engine Performance in a Steady-state Condition

Figure 12 shows the calculated and experimentally obtained heat release rates. This figure indicates that the calculation results agree with the experimental results for low to high loads. Therefore, this simulation model has a very wide range of engine performance prediction.

Figure 13 shows the calculated and experimentally obtained combustion noise levels. The results are shown as contour maps. Since the predicted heat release rate agrees with the experimental results, the predicted noise level also agrees with the experimental results.

Figure 14 shows the results for the calculated and experimental NOx emission. The accuracy of the NOx prediction is somewhat low in some cases. However, in general, the amount of predicted NOx agrees well with the experimentally obtained results.

4. 4 Prediction of Multi-cylinder Engine Performance in a Transient Condition

The vehicle, driver, and ECU models were linked, and transient calculations for the NEDC were conducted. Vehicle speed and gear shift instructions conforming to the NEDC regulations were provided as external inputs, and a fully warmed-up condition was assumed.

The results are shown in **Fig. 15**. The engine was kept running at the target speed by the accelerator control in the driver model. The predicted fuel injection quantity behavior was approximately equivalent to the

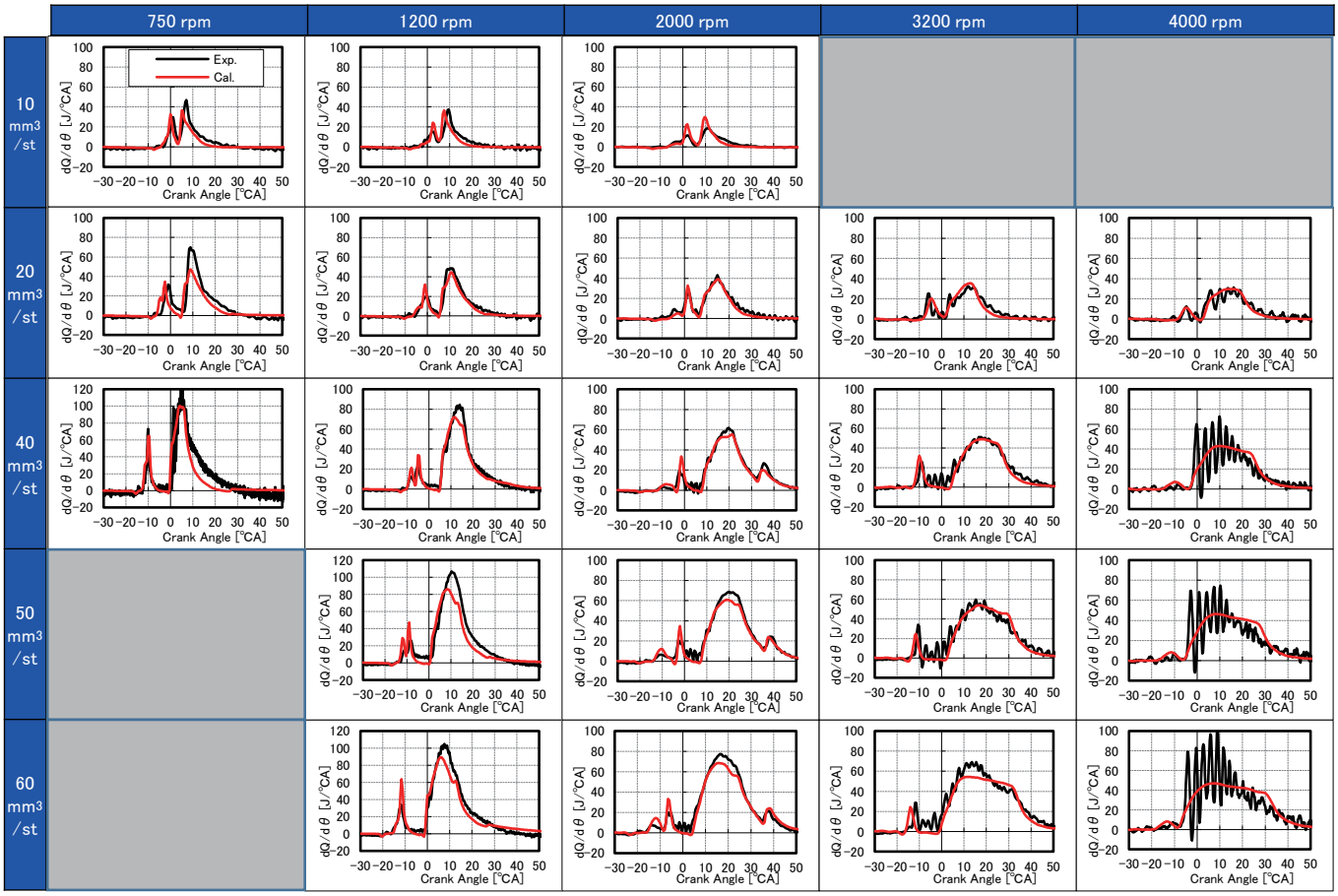

Fig. 12 Comparison of heat release rate between experiment and calculation.

© Toyota Central R&D Labs., Inc. 2014

experimental results. The intake manifold pressure and exhaust manifold temperatures were also equivalent to the experimental results.

The transient and steady-state calculations were compared as follows. **Figure 16** shows the combustion indicated by (A) in Fig. 15 and the steady-state results calculated at the same engine speed and load conditions. In this steady-state calculation, the total vehicle model with a steady-state condition of 1476 rpm and 25.3 mm^3/st. was used. As shown in Fig. 16, the combustion was different for these two conditions. The reason for this difference is considered to be the higher cylinder pressure, lower temperature, and lower O_2 concentration at the first pilot injection timing shown in **Table 3**. **Figure 17** shows the transient condition around position (A) in Fig. 15. During the acceleration period, the fuel was injected, so that the intake pressure was also kept high by a turbo charger. However, the O_2 concentration of the intake gas was kept low due to the EGR. During the shift change, fuel cut-off was caused by the throttle pedal setting. The intake pressure did not decrease instantaneously due to the turbine inertia. Moreover, the exhaust gas in the intake manifold was scavenged. The fuel was reinjected at (A) in Fig. 15. At (A), the intake pressure was kept high, the O_2 concentration was high, and the gas temperature was low due to the low EGR in the intake manifold. In this way, the transient condition is different from the steady-state condition due to the transient change of the turbo charger and EGR, for example.

A number of values in an engine system are difficult to measure in a transient condition. However, this total vehicle model is capable of predicting these value, so that this model is a very useful tool.

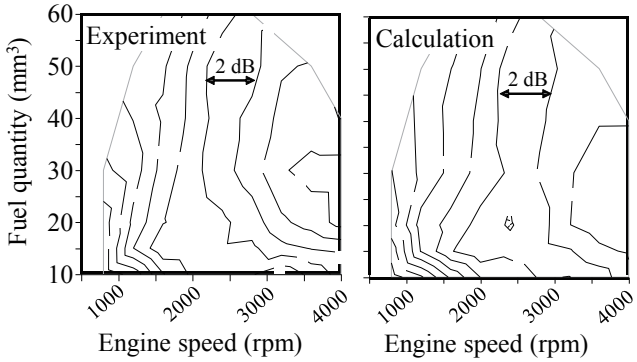

Fig. 13 Comparison of combustion noise map between experiment and calculation.

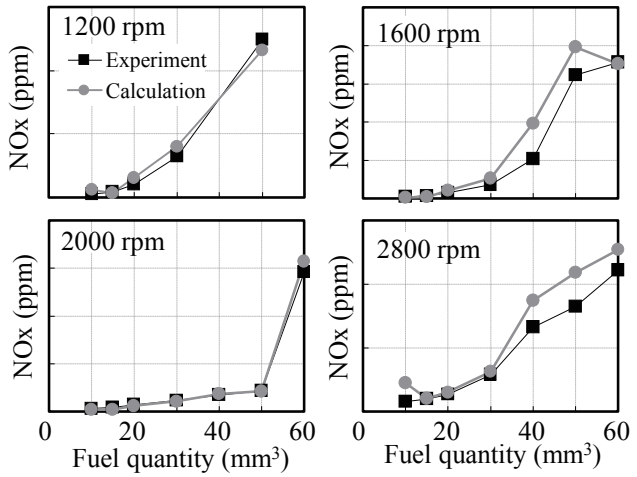

Fig. 14 NOx predictability in change of fuel quantity (1200, 1600, 2000, 2800 rpm).

5. Conclusion

A diesel combustion model (UniDES) that is capable of predicting the transient performance of a diesel engine was investigated. This model uses a multi-zone model and a probability density function (PDF). Seven injections are treated as seven zones in UniDES, and the interaction between sprays is treated as the interaction between zones.

The addition of a novel nozzle sac pressure estimation and adjacent spray interaction models to the combustion model made it possible to apply the simulation to a broad range of operating conditions ranging from low to high loads.

Trends for heat release rate, NOx emissions, and combustion noise could be predicted under steady-state operating conditions in relatively frequent operating ranges. The combustion model, GT-POWER® engine model, and the ECU model were combined. The NEDC was investigated as an example of a transient condition application. It was possible to perform a detailed analysis of the transient behavior of the gas, control, and combustion state in a fully warmed-up state.

This combustion model is capable of predicting engine performance in both static and transient conditions without using a real engine or vehicle. As a result, the UniDES model is a very useful tool for developing new engines and vehicles.

© Toyota Central R&D Labs., Inc. 2014

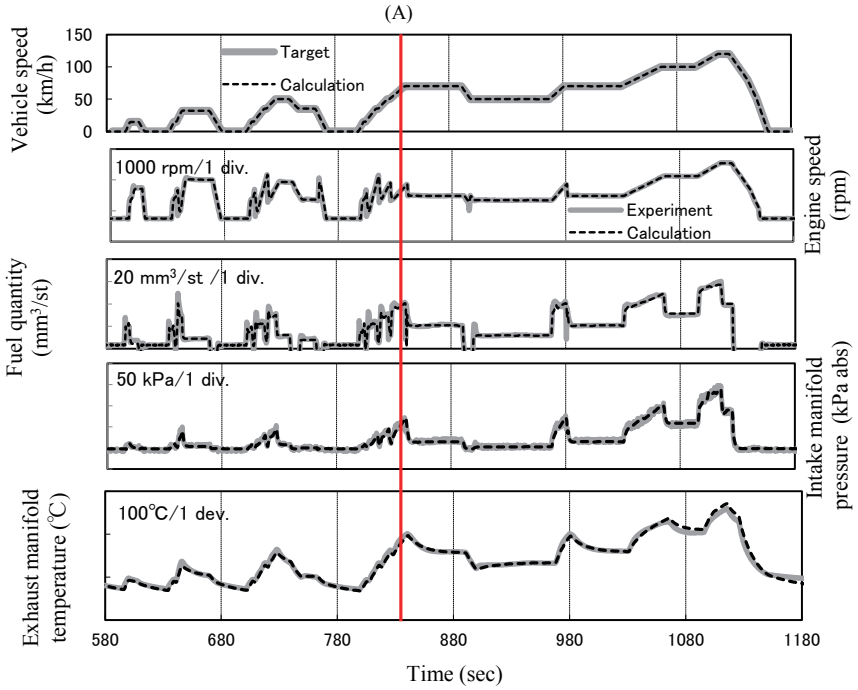

Fig. 15 Simulation results of NEDC transient condition (hot condition).

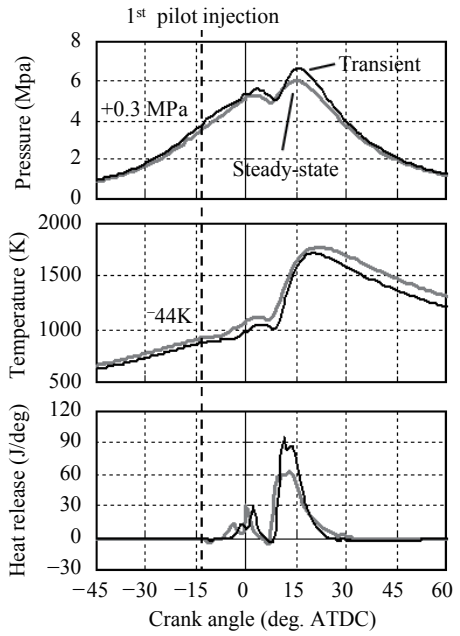

Fig. 16 Comparison of combustion in transient and steady-state conditions (1476 rpm, 25.3 mm³/st, position (A) in Fig. 15).

Table 3 Engine states after fuel-cut at position (A) in Fig. 15 (1476 rpm, 25.3 mm³/st).

Cylinder status	Deviation form steady-state
Pressure	+0.3MPa@ 1st pilot injection
Temperature	-44K@ 1st pilot injection
O^2 concentration	+2.3%

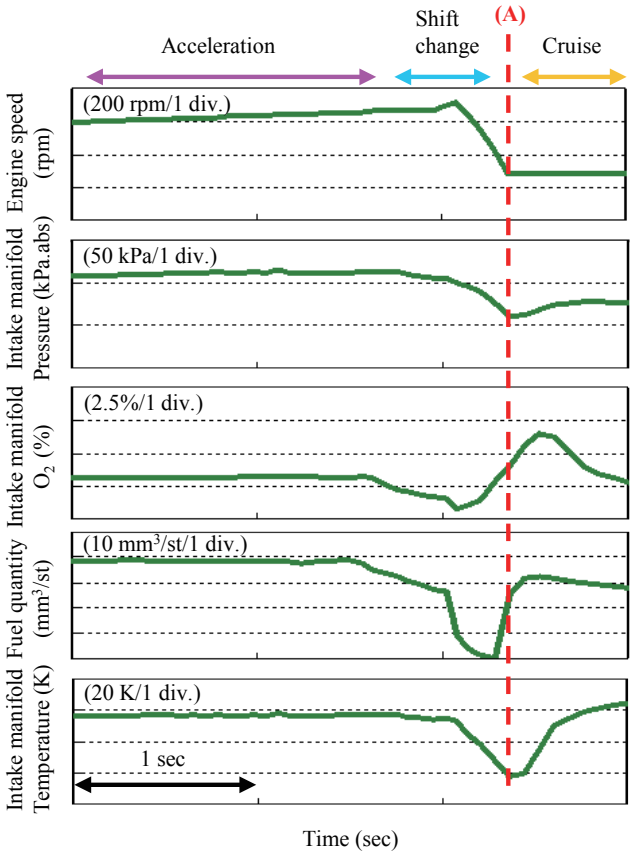

Fig. 17 Analysis of transient conditions around position (A) in Fig. 15.

© Toyota Central R&D Labs., Inc. 2014

REFERENCES

(1) Yamashita, A. et al., "Development of Low Pressure Loop EGR System for Diesel Engines", *SAE Tech. Paper Ser*., No. 2011-01-1413 (2011).
(2) Alano, E. et al., "Compact SCR for Passenger Cars", *SAE Tech. Paper Ser*., No. 2011-01-1318 (2011).
(3) Ueda, M. et al., "The Present and Future Control of the Automobile Diesel Engine", *Engine Technology Review*, Vol. 1, No. 3 (2009), pp. 42-47.
(4) Benjamin, A. et al., "Strategies for Reducing the Computational Time Required for Diesel Engine Simulations with KIVA", *Proc. of COMODIA* (2012), pp. 554-559.
(5) Inagaki, K. et al., "Universal Diesel Engine Simulator (UniDES):1st Report: Phenomenological Multi-zone PDF Model for Predicting the Transient Behavior of Diesel Engine Combustion", *SAE Tech. Paper Ser*., No. 2008-01-0843 (2008).
(6) Minako, A. et al., "A Phenomenological Combustion Model for Heat Release Rate Prediction in High-speed DI Diesel Engines with Common Rail Injection", *SAE Tech. Paper Ser*., No. 2000-01-2933 (2000).
(7) Takasu, Y. et al., "Universal Diesel Engine Simulator (UniDES) 2nd Report: Prediction of Engine Performance in Transient Driving Cycle Using One Dimensional Engine Model", *SAE Tech. Paper Ser*., No. 2013-01-0881 (2013).
(8) Inagaki, K., "A Phenomenological Multi-zone PDF Model to Predict Transient Behavior of Diesel Engine Combustion", *R&D Review of Toyota CRDL*, Vol. 42, No. 4 (2011), pp. 73-82.
(9) Hiroyasu, H. et al., "Models for Combustion and Formation of Nitric Oxide and Soot in Direct Injection Diesel Engines", *SAE Tech. Paper Ser*., No. 760129 (1976).
(10) Hiroyasu, H. et al., "Fuel Spray Penetration and Spray Angle in Diesel Engine (in Japanese with English summary)", *JSAE Trans*., No. 21 (1980), pp. 5-11.
(11) Ziejewski, M. et al., "Discharge Coefficients for Multi-hole Fuel Injection Nozzle for Alternate Fuels," SAE Tech. Paper Ser., No. 890448 (1989).
(12) Kawamura, K, et al., "Analysis of Fuel Spray Characteristics Under High Pressure Injection", *JSAE*, Vol. 23, No. 24 (1992), pp. 20-24.
(13) Spalding, D. B., "The combustion of liquid fuels", *Proc. of 4th Symp. (Int.) on Combustion* (1952), pp. 847-864.
(14) Halsted, M. P. Kirsch. et al., "The Autoignition of Hydrocarbon Fuels at High Temperatures and Pressures-fitting of a Mathematical Model'', *Combution and Flame*, Vol. 30 (1977), pp. 45-60.
(15) Kong, S. C. et al., "The Development and Application of a Diesel Ignition and Combustion Model for Multidimensional Engine Simulation", *SAE Tech. Paper Ser*., No. 950278 (1995).
(16) Ikegami, M. et al., "A Stochastic Approach to Model the Combustion Process in Direct-injection Diesel Engines", *20th Symp. (Int.) on Combustion* (1984), pp. 217-224.
(17) Murakami, A. et al., "Swirl Measurements and Modeling in Direct Injection Diesel Engines", *SAE Tech. Paper Ser*., No. 880385 (1988).

Fig. 2
Reprinted from Proc. of the 21st Int. Combustion Eng. Symp. (2010), pp. 309-314, © 2010 JSAE.

Figs. 3, 4 and 7-9
Reprinted and modified from Proc. of JSAE Annual Congress (Spring) (2011), 20115037, © 2011 JSAE, with permission from Society of Automotive Engineers of Japan.

Figs. 5, 10, 11, 13 and 14
Reprintedfrom Proc. of JSAE Annual Congress (Spring) (2012), 20125141, © 2012 JSAE, with permission from Society of Automotive Engineers of Japan.

Figs. 6, 16 and Tables 1-3
Reprinted and modified from Proc. of JSAE Annual Congress (Fall) (2011), 20115673, © 2011 JSAE, with permission from Society of Automotive Engineers of Japan.

Fig. 17
Reprinted from SAE Tech. Paper Ser., No. 2013-01-0881 (2013), © 2013 SAE, with permission from SAE International.

Matsuei Ueda
Research Fields:
- Diesel Engine Combustion
- Exhaust Aftertreatment System

Academic Degree: Dr.Eng.
Academic Societies:
- Society of Automotive Engineers of Japan
- The Japan Society of Mechanical Engineers

Award:
- Outstanding Technical Paper Award of JSAE, 2004 and 2010

Kazuhisa Inagaki
Research Field:
- Diesel Engine Combustion

Academic Degree: Dr.Eng.
Academic Societies:
- Society of Automotive Engineers of Japan
- The Japan Society of Mechanical Engineers

Awards:
- Outstanding Technical Paper Award of JSAE, 2004, 2005, 2009, 2010 and 2012
- Best Presentation Award of JSAE, 2013
- SAE Horning Memorial Award, HARRY LEVAN, 2003

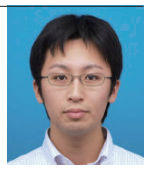

Yusuke Takasu*
Research Field:
- Diesel Engine Simulation

Academic Society:
- Society of Automotive Engineers of Japan

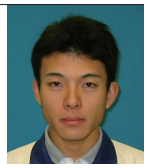

Toshihiro Tani**
Research Field:
- Diesel Engine Combustion

Academic Society:
- Society of Automotive Engineers of Japan

* TOYOTA MOTOR CORPORATION
** TOYOTA INDUSTRIES CORPORATION

© Toyota Central R&D Labs., Inc. 2014